Article

Iridium Azocarboxamide Complexes: Variable Coordination Modes, C−H Activation, Transfer Hydrogenation Catalysis, and Mechanistic Insights

Shubhadeep Chandra, Ola Kelm, Uta Albold, Arijit Singha Hazari, Damijana Urankar, Janez Košmrlj,* and Biprajit Sarkar*

Read Online

ACCESS | Metrics & More | Article Recommendations | Supporting Information

ABSTRACT: Azocarboxamides, a special class of azo ligands, display intriguing electronic properties due to their versatile binding modes and coordination flexibility. These properties may have significant implications for their use in homogeneous catalysis. In the present report, half-sandwich Ir−Cp* complexes of two different azocarboxamide ligands are presented. Different coordination motifs of the ligand were realized using base and chloride abstracting ligand to give N^N-, N^O-, and N^C-chelated monomeric iridium complexes. For the azocarboxamide ligand having methoxy substituted at the phenyl ring, a mixture of N^C-chelated mononuclear (**Ir-5**) and N^N,N^C-chelated dinuclear complexes (**Ir-4**) were obtained by activating the C−H bond of the aryl ring. No such C−H activation was observed for the ligand without the methoxy substituent. The molecular identity of the complexes was confirmed by spectroscopic analyses, while X-ray diffraction analyses further confirmed three-legged piano-stool structure of the complexes along with the above binding modes. All complexes were found to exhibit remarkable activity as precatalysts for the transfer hydrogenation of carbonyl groups in the presence of a base, even at low catalyst loading. Optimization of reaction conditions divulged superior catalytic activity of **Ir-3** and **Ir-4** complexes in transfer hydrogenation over the other catalysts. Investigation of the influence of binding modes on the catalytic activity along with wide range substrates, tolerance to functional groups, and mechanistic insights into the reaction pathway are also presented. These are the first examples of C−H activation in azocarboxamide ligands.
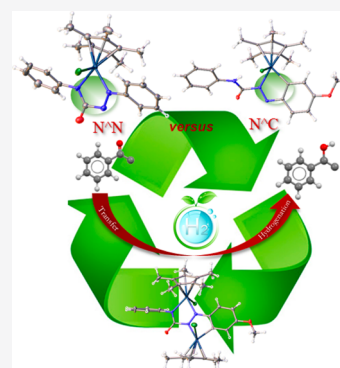
1. INTRODUCTION

Azocarboxamides, a special class of multifaceted redox-active azo chelating ligands have garnered considerable attention by virtue of its diverse coordination modes, and redox activity.[1−3] The azo group (−N=N−) in the azocarboxamide ligand is surrounded by a carbonyl oxygen of the amide group, which can potentially be used as a donor atom along with the nitrogen atom of the azo group (N^O-chelated ring, Chart 1).

Chart 1. Different Coordination Modes of Azocarboxamide Ligand and the Ligands Used in This Work
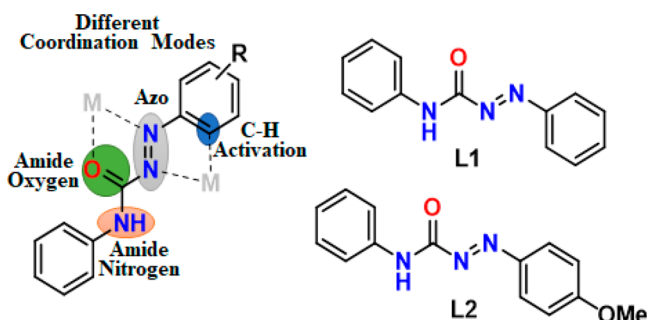
Furthermore, in the presence of a base, the azocarboxamide ligand can also bind to a metal center via the deprotonated nitrogen atom of the amide together with the nitrogen atom of the azo group (N^N-chelated ring).[1,3] Interestingly, it can also provide an additional binding pocket to the metal center by activating the C−H bond from one of the phenyl rings. This depends on the functionalization of the phenyl ring and the electronic properties of the metal center and its ancillary ligands, leading to the formation of the stable five-membered cyclometalated complex (N^C-chelated ring). While examples of the first two coordination modes are already available in the literature for ruthenium complexes,[1−3] the latter cyclo-metalated coordination mode is not reported for azocarbox-amide ligands.

The aforementioned possible coordination mode via the amide oxygen, the nitrogen atoms of the azo group and the
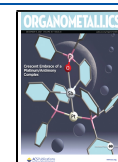
activated C−H bond should further allow the formation of a bimetallic complex, in which one of the metal centers coordinates via one of the nitrogen atoms from the azo group and the amide nitrogen forming the N^N chelate ring, while the other metal center binds through the second nitrogen atom from the azo group and the orthometalation of the phenyl ring to form N^C chelate ring. This type of cyclometalated bimetallic complex has never been observed with azocarboxamide ligands. Moreover, such a coordination mode, in which a cyclometalated bridging ligand provides two different binding modes for two metals within the same ligand framework, is generally rare.

While other azo-containing ligands such as pap (phenyl-azopyridine) and azobispyridine have been extensively studied in coordination chemistry as redox-active bridging ligands,[4−8] azocarboxamides, a special class of azo-containing ligands, have rarely been used in coordination chemistry and for the study of redox as well as catalytic properties. A recent report on ruthenium azocarboxamide half-sandwich complexes from our group illustrated the redox-triggered change in the chelating binding pocket and the electronic properties of the complexes.[2] We have also investigated the antitumor activity of ruthenium azocarboxamide complexes.[3] In addition, the effect of the position and protonation state of the amide group on the catalytic activities of their ruthenium complexes has also been described.[1]

Transfer hydrogenation has emerged as a versatile protocol for the reduction of unsaturated molecules containing C=C, C=N, and C=O double bonds.[9−13] In past decades, considerable effort has gone into the development of new transfer hydrogenation catalysts based on transition metals that use readily available hydrogen donors such as isopropanol or formic acid, thereby avoiding the use of hazardous hydrogen gas under high pressure or the stoichiometric amount of strong reducing agents. A wide range of iridium complexes with various chelating ligands such as carbenes,[14−16] and bipyr-idine[17] leading to the formation of N^C and N^N chelate ring, have been extensively studied for transfer hydrogenation catalysis.[18−21] In contrast, the N^O-chelated half-sandwich iridium complexes derived from different α- and β-amino acids are rarely used in catalysis,[22−24] despite their importance from the synthetic and structural viewpoint.

In view of the effect of variable binding modes of the azocarboxamide ligand on the electronic and structural properties, we present here the synthesis and catalytic behavior of N^N,N^C-chelated or N^O-chelated half-sandwich Ir(III) complexes (Chart 2). The effect of additional functional groups on the phenyl substituents of the azocarboxamide ligands (L1 vs L2) on the C−H activation of the resulting metal complexes is investigated. In addition to the mono-metallic complexes, we report the first example of a bimetallic iridium complex with azocarboxamide ligand L2, in which two iridium centers are coordinated to the ligand in an unusual coordination mode. Electronic and geometric structures of these metal complexes are also discussed. Furthermore, strong effects of the variable mode of chelation on the transfer hydrogenation of carbonyl groups is demonstrated. The overall coordination diversity of azocaboxamides is explored, and the effect of the different coordination modes on the transfer hydrogenation efficiency of the resulting complexes is demonstrated.

Chart 2. Coordination Modes of Azocarboxamides Targeted in This Work
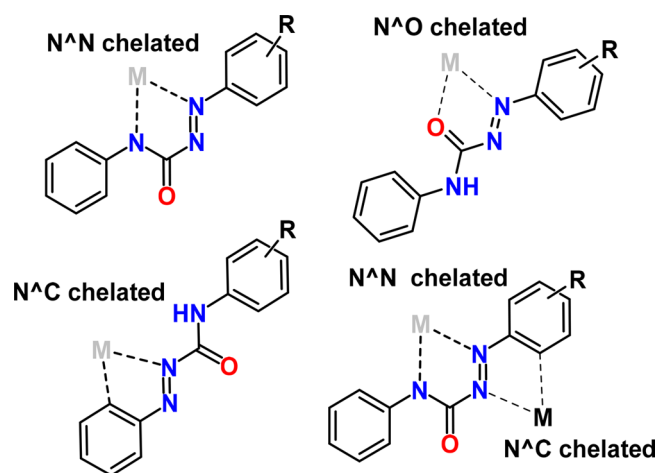
2. RESULTS AND DISCUSSION

2.1. Synthesis and Characterization. Deprotonation of ligand **L1** with trimethylamine NEt$_3$ and subsequent reaction with [Cp*IrCl$_2$]$_2$ at room temperature gave green-colored complex **Ir-1**. While the presence of a base led to the formation of a neutral complex, reaction of **L1** with [Cp*IrCl$_2$]$_2$ in the presence of the chloride-abstracting reagent NH$_4$PF$_6$ under reflux conditions led to the formation of cationic complex **Ir-2** (Scheme 1). Both complexes are stable in air and were purified

Scheme 1. Synthesis of Iridium Complexes Ir-1 and Ir-2
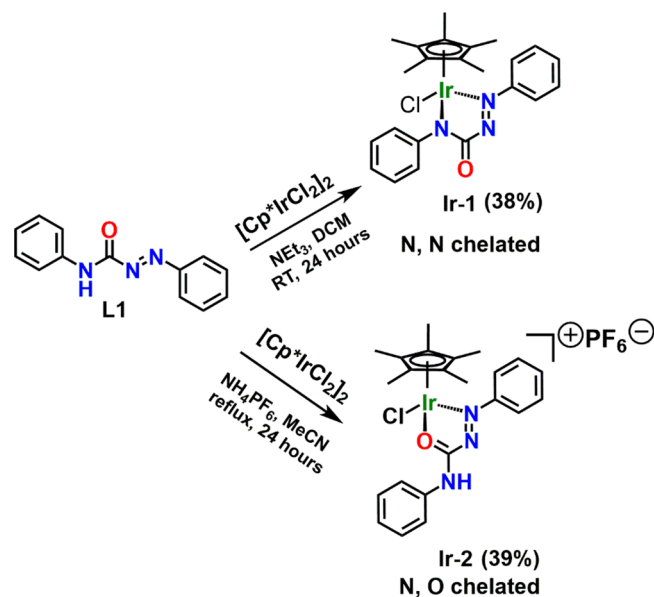
by column chromatography over neutral alumina followed by crystallization from a mixture of dichloromethane and hexane. Under these reaction conditions, no activation of the C−H bond of the phenyl ring was detected, even after a prolonged reaction time. The two complexes were characterized by various spectroscopic techniques such as NMR and mass spectrometry.

In the case of **Ir-1**, the ^{1}H NMR signals corresponding to the aromatic protons (7.95−7.15 ppm) and the singlet of the methyl groups of the coligand Cp* (1.22 ppm) are shifted to

the high-field region compared to the starting materials (Figure S3). The disappearance of the signal corresponding to the −NH proton of the free ligand at 8.45 ppm indicates the deprotonation and subsequent coordination to the metal through the amide nitrogen (N^N-chelated). The ^{1}H NMR spectrum of complex **Ir-2** shows multiplets in the range of 8.41−7.19 ppm due to the aromatic protons of the phenyl ring and a singlet at 1.75 ppm for the methyl groups of the coligand Cp* (Figure S4). Compared to those of complex **Ir-1**, all the resonances of **Ir-2** are shifted significantly downfield. The presence of the amide NH signal at 9.56 ppm suggests that the ligand is coordinated to the iridium through the desired N^O coordination motif. Moreover, NMR studies (in CDCl$_3$) in the presence of a base (NEt$_3$) reveal that **Ir-2** can be converted to **Ir-1** as evident from the gradual disappearance of the amide− NH signal at 9.56 ppm with the progress of the reaction (Figure S17).[3]

Cyclometalated complex **Ir-5** was obtained by treating of **L2** with [Cp*IrCl$_2$]$_2$ in the presence of NH$_4$PF$_6$ at elevated temperature (Scheme 2). The ^{1}H NMR spectrum of **Ir-5**

Scheme 2. Synthesis of Iridium Complexes Ir-3, Ir-4, and Ir-5
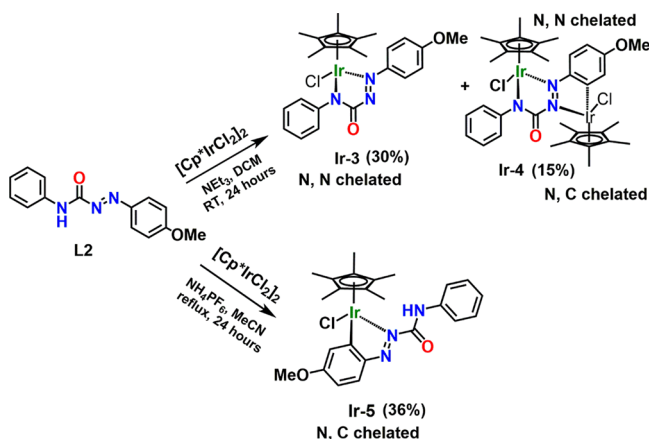
features one resonance for the NH proton at 9.57 ppm and three distinct resonances for the C-bonded aryl C−H protons, in addition to five aryl C−H resonances for the phenyl ring, indicating N,C-coordination instead of the usual N,O-coordination of the ligand (Figure S7). The ^{13}C{1H} NMR spectrum shows the resonance for the cyclometalated carbon atom at 163 ppm, which is significantly shifted to the downfield region compared to the other carbon resonances (Figure S7).

On treating **L2** with [Cp*IrCl$_2$]$_2$ in the presence of a base at room temperature under the same reaction conditions as for complex **Ir-1**, a mixture of two complexes **Ir-3** and **Ir-4** was obtained in 30 and 15% yields, respectively (Scheme 2). All attempts to exclusively synthesize one of the products failed and gave the mixture of both complexes. However, both complexes are stable in air and could be separated by column chromatography over neutral alumina. All complexes were unambiguously characterized by NMR spectroscopy. The ^{1}H NMR spectrum of red-colored complex **Ir-4** shows two distinct resonances for the methyl groups of the coligand Cp* at 1.82 and 1.29 ppm in a 1:1 ratio and only eight instead of nine resonances for aromatic C−H protons in the aromatic region at 8.39−6.84 ppm, indicating the activation of the C−H bond

of the phenyl ring (Figure S6). Moreover, the disappearance of the resonance of the −NH proton of the free ligand at 8.45 ppm clearly suggests the formation of a binuclear complex in which the metal centers are bridged through N,N-donor atoms on one side of the binding pockets and N,C-donor atoms on the other side. The ESI mass analysis in a positive mode also confirmed the formation of the binuclear complex, showing a molecular peak at m/z 944.2141.

The ^{1}H NMR spectrum of green-colored complex **Ir-3** shows the resonances expected for the desired mononuclear complex for the ligand in the aromatic region at 8.02−6.98 ppm, and the singlet for the methoxy group at 3.92 ppm. The singlet for the methyl groups of the coligand Cp* is shifted to the high field at 1.26 ppm compared to the precursor. The absence of the NH signal at 8.45 ppm indicates N,N-coordination of the ligand to the metal center (Figure S5).

The ^{1}H NMR chemical shift as a measure of the C−H acidity of the respective C−H proton for ligands **L1** and **L2** could be considered as a simplified useful tool to distinguish their different reactivities toward C−H bond activation. Recently, Steel and co-workers reported a good correlation between the ^{1}H NMR chemical shift as a measure of C−H acidity and the preferential site selectivity of iridium-catalyzed borylation of C−H bonds.[25,26] Thus, the resonance of the corresponding C−H proton in **L2** (δ = 8.04 ppm) shifted slightly to lower fields than the C−H proton of the corresponding **L1** (δ = 7.95), leading to the formation of cyclometalated complexes **Ir-4** and **Ir-5**. Therefore, the activation of the C−H bond by the "Ir^{III}−Cl" motif through a concerted metalation−deprotonation process similar to σ-bond metathesis could be considered as a plausible mechanism for the activation of the more acidic C−H protons in the case of ligand **L2**, with the chloride ligand acting as an internal base to deprotonate the C−H protons (Figure 1).[27,28] The electron
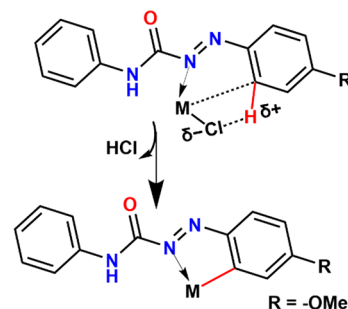
Figure 1. Schematic for the concerted metalation−deprotonation mechanism for C−H bond activation.

density on the iridium center, the Ir−C$_{aryl}$ bond strength, as well as the basicity of the chloride ion could also play a role for their different reactivity toward C−H activation.[26]

2.2. X-ray Diffraction. Three of the complexes were structurally characterized by single-crystal X-ray diffraction. Single crystals suitable for the diffraction studies were obtained by diffusion of concentrated solutions of the sample in a dichloromethane/hexane solvent mixture at ambient temperature. The crystallographic data and relevant binding parameters for all complexes are collected in Table 1. Analysis of the structural data of all the complexes reveals the formation of five-membered iridacycle in each of the complexes with the iridium(III) center coordinated to nitrogen or oxygen donor atoms of azo/amide groups along with the ortho-metalated C$^−$

Table 1. Selected Bond Lengths and Bond Angles in Complexes Ir-1, Ir-4, and Ir-5

	bond lengths			bond angle					
bond	Ir-1	Ir-4	Ir-5	Ir-1		Ir-4		Ir-5	
Ir1−N1	2.059(8)	2.061(4)	2.048(3)	N1−Ir1−N3	74.5(3)	N1−Ir1−N3	74.09(16)	N1−Ir1−C8	76.1(12)
Ir1−N3	2.059(8)	2.070(4)		N2−N3−Ir1	120.6(6)	C1−N3−Ir1	117.7(3)	C14−C8−Ir1	112.8(2)
Ir−C8			2.030(3)	N1−C1−N2	113.9(8)	N2−N1−Ir1	118.7(3)	N1−N2−C14	111.4(3)
Ir2−C13		2.008(5)		N3−N2−C1	112.2(8)	N1−N2−Ir2	118.7(3)	N2−C14−C8	118.5(3)
N1−N2		1.293(6)	1.294(4)	C1−N1−Ir1	116.9(6)	N2−Ir2−C13	77.56(18)	N2−N1−Ir1	121.1(2)
N2−N3	1.276(11)					C8−C13−Ir2	113.5(3)		
C1−O1	1.226(12)	1.226(6)	1.211(4)			N3−C1−N2	111.8(4)		
C1−N1	1.334(13)		1.456(4)			C1−N2−N1	114.2(4)		
C1−N2	1.468(13)	1.461(6)							
C1−N3		1.334(6)	1.349(4)						
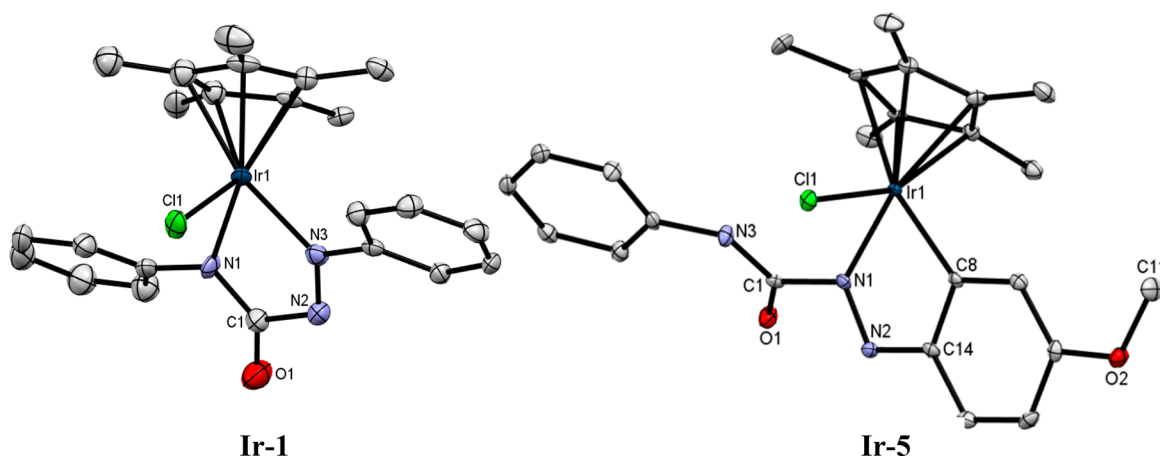
Figure 2. ORTEP representation of complexes **Ir-1** and **Ir-5**. Ellipsoids are drawn at 50% probability level. Hydrogen atoms and solvent molecules are omitted for clarity.

center of the aryl ring. The crystal structures of all complexes exhibit typical half-sandwiched three-legged piano-stool geometry, with the η^5-Cp* ring occupying the seat of the piano stool, with N_{azo}/N_{amide}, O_{amide} donor, C_{aryl} donor, and Cl donor atoms imitating three legs of the stool. All complexes show similar metric parameters within a limit of experimental standard deviation. Consistent with Ir(III)−Cp* complexes reported in the literature, the Cp* ring is coordinated to the central Ir(III) atom in an η^5 fashion, with the distance between the centroid of the Cp* ring and Ir(III) falling within the range of 1.794−1.834 Å in all complexes. Depending on the N N_{azo}/N_{amide} donor and C_{aryl} donor atoms of the azocarboxamide ligand, the variable binding pockets are formed in the three complexes. In complex **Ir-1**, the chelating ligand is bound to the central metal atoms through the N donor atoms of the azo group along with the deprotonated N donor atoms of the amide moiety forming a five-membered chelate ring (Figure 2). However, a five-membered chelate ring in complex **Ir-5** consists of Ir(III) attached to the azocarboxamide ligand through N_{azo} and C_{aryl} donor atoms, respectively. In dinuclear complex **Ir-4** (Figure 3), two five-membered iridacycles are formed, in which the N_{azo} and N_{amide} donor atoms coordinate to the Ir on one side, while N_{azo} and aryl carbon atom of the phenyl ring bind to the Ir on the other side. The distance between the Ir⋯Ir centers in the dinuclear complex is 4.830 Å, which is relatively shorter than that in the reported dinuclear complexes of Ir(III)−Cp*.[29] The N−N bond distances of the coordinated azo group are in the range of 1.276−1.294 Å, deviating slightly from the free ligand and indicating an
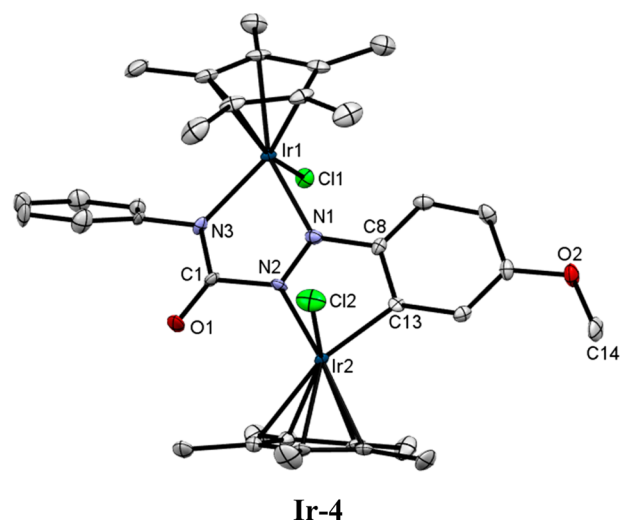
Figure 3. ORTEP representation of dinuclear complex **Ir-4**. Ellipsoids are drawn at 50% probability level. Hydrogen atoms and solvent molecules are omitted for clarity.

unreduced form of the ligand.[3] The C−N bond distances, however, vary quite significantly (1.334−1.461 Å) among the three different complexes, which could be attributed to the delocalization of charge due to the deprotonation of the NH group of the amide. In contrast, the C−O bond distances in all the complexes are in the range of 1.21−1.22 Å, which is almost equal to the free C═O bond length. The bite angle around the

Ir center from the N^N and N^C chelate lies in the range of 74.5−76°.[30] While the Ir-center in complex **Ir-1** is almost coplanar with the ligand, the phenyl ring deviates by a torsion angle of 32.63°. Furthermore, the phenyl group containing the carboxamide is twisted from the chelating plane by ∼44°. In the cyclometalated dinuclear Ir complex, one of the Ir-centers is twisted by 15.40° from the plane of the azocarboxamide. Analysis of the binding parameters around the coordination environment of Ir in complex **Ir-4** clearly establishes its identity as an *anti*-isomer. Thus, the X-ray structural parameters of all complexes clearly demonstrate the molecular variable binding modes of the azocarboxamide ligand in three different cyclometalated Ir(III)−Cp* complexes.

2.3. Electrochemistry and Transfer Hydrogenation.

Complex **Ir-2** shows irreversible reduction at −1.51 V, in addition to quasi-reversible oxidation at 0.66 V (Figure 4). In
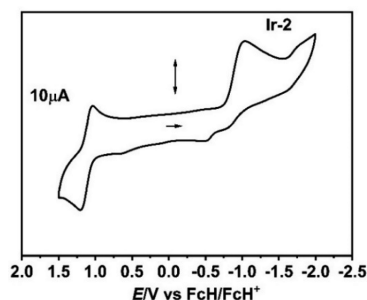
Figure 4. Cyclic voltammogram of **Ir-2** in DCM/0.1 M Bu₄NPF₆.

complex **Ir-1**, both the oxidation and reduction processes are irreversible (Figure S1). The irreversible reduction process is likely a ligand-centered process considering the free radical EPR signal without hyperfine coupling with a *g* value of 2.038 at 298 K (Figure S2) obtained for the one-electron-reduced form of complex **Ir-1**. Moreover, as reported in previous publications from our group, the free ligand (**L1**) exhibits an irreversible reduction process at −1.33 V, which indeed supports a ligand-centered reduction process in the complexes.[1−3] The irreversible reduction and oxidation processes indicate the involvement of an electron-transfer/chemical reaction (EC) mechanism with the elimination of chloride ion for the reduction and possible ligand rearrangement for the oxidation processes.

Whereas no oxidative process was observed in a previously studied corresponding ruthenium complex,[3] iridium complex **Ir-2** shows a quasi-reversible oxidation process which could be related to the presence of the negatively charged coligand Cp*. In addition, the negatively charged coligand stabilizes higher oxidation states of iridium. The redox behavior of iridium complex **Ir-3** is similar to that of complex **Ir-1** with one irreversible reduction at −1.25 V with three small reoxidation waves occurring in response to the first reduction (Figure S1). In contrast to mononuclear complex **Ir-3**, binuclear **Ir-4** iridium complex shows two irreversible reductions at −1.15 and −1.97 V, respectively (Table S2).

The catalytic properties of iridium complexes **Ir-1**−**Ir-5** were studied in the transfer hydrogenation of carbonyl groups to investigate the effects of their different binding modes and the ligand substituents at the azocarboxamide ligands **L1** and **L2**. Benzophenone was chosen as the model substrate, isopropanol was used as the both hydrogen source and solvent. KOH was used as the base to optimize the critical

reaction parameters. Under N₂ atmosphere, a solution of benzophenone and 1 mol % of catalyst in the presence and absence of 10 mol % KOH was heated to 100 °C for 20 h.

In the absence of a base, all complexes showed almost no catalytic activity in transfer hydrogenation. As can be seen from Table 2, in the presence of base and 1 mol % catalyst loading,

Table 2. Comparison of Activities of Different Catalyst[a]

entry	catalyst	loading/mol %	time/h	base/mol %	conversion/%
1	**Ir-1**	1	20	10	84
2	**Ir-2**	1	20	10	75
3	**Ir-3**	1	20	10	>99
4	**Ir-4**	1	20	10	>99
5	**Ir-4**	0.5	20	10	>99
6	**Ir-4**	0.25	20	10	70
7	**Ir-5**	1	20	10	60
8	**Ir-3**	0.5	20	10	97
9	**Ir-3**	0.5	12	10	65
10	**Ir-3**	0.5	20	5	65

[a]Reaction conditions: benzophenone (0.25 mmol) in 3 mL of isopropanol at 100°C, catalyst precursor (0.5−1 mol %), base (5−10 mol %). Yield measured by ¹H NMR spectroscopy using hexamethylbenzene as an internal standard.

benzophenone could be reduced by all complexes. Significantly different catalytic activity was observed for the different iridium complexes.

Both N^O- and N^N-chelated iridium complexes **Ir-1** and **Ir-2** showed nearly identical activity, achieving only about 80% conversion within 20 h at a catalyst loading of 1 mol %. It is known from our previous report that in similar ruthenium complexes, the N^O-chelated complex could be converted to the N^N-chelated complex by the addition of base.[3] Therefore, the identical activity of the N^O- and N^N-chelated iridium complexes could be attributed to the formation of the same active species by the reaction of **Ir-1** and **Ir-2** with base.

While N^N-chelated iridium complex **Ir-1** showed only 80% conversion after 20 h, complex **Ir-3** (N^N), which is the analog of **Ir-1**, exhibited much higher activity and offered almost quantitative conversion after 20 h. The activity of **Ir-3** was found to be higher than that of **Ir-1**. In the case of **Ir-3**, the presence of the electron-donating methoxy group makes the iridium center more electron-rich compared to **Ir-1**, therefore the difference in activity between **Ir-1** and **Ir-3** upon transfer hydrogenation could be explained by the higher electron density at the iridium center in **Ir-3**, which normally facilitates the formation of the metal hydride species.[31] The bimetallic complex **Ir-4**, containing both N^N and N^C donor sets, also showed high catalytic activity and near-quantitative conversion after 20 h even at 0.5% catalyst loading. The high reactivity of complex **Ir-4** is likely related to the presence of the amide chelating pocket in this complex. The lowest activity was observed for mononuclear cyclometalated iridium complex **Ir-5** with a chelating carbon donor (N^C donor), which gave only 60% conversion after 20 h.

The correlation derived from the NMR experiments between the different coordination mode for iridium complexes and the catalytic activity clearly suggests that the

catalytic activity could be modified by improving the ligand donor properties and also by modifying the second coordination site.[32] It is known that the reactivity of catalysts for the reduction of ketones can be improved by introducing an N−H unit in the ligand in close proximity to the active metal center, which can lower the barrier of the transition state through a hydrogen bonding network.[33]

In the case of **Ir-5**, the amide group is not directly connected to the metal center, which may be the reason for the lower catalytic activity.[24] Moreover, conversion between the two different coordination modes in the presence of a base, as suggested for **Ir-1** and **Ir-2**, is probably not possible here because of the strength of the Ir−C bond to the cyclometalated phenyl group.

Further optimization of base, reaction time, and catalyst loading was carried out with **Ir-3** and **Ir-4**, which showed the highest activity among all iridium complexes. The higher activity of **Ir-3** and **Ir-4** could possibly be ascribed to the bifunctional feature of the iridium azocarboxamide catalyst resulting in the facile activation of the isopropanol which is reported previously by Ikariya and co-workers.[34] Identical reactivity was observed for **Ir-3** and **Ir-4** when using 0.5 mol % loading. Both complexes showed almost complete conversion after 20 h. In the case of **Ir-4**, the catalyst performance decreased when the amount of catalyst was further reduced to 0.25 mol %, resulting in a conversion of only 70% after 20 h. This observation likely points to the fact that the N,N binding pocket containing the amide donor as in **Ir-3** is the most important structural motif for achieving high catalytic activity. The amount of base had a significant effect on the catalytic activity. Decreasing the amount of base from 10 to 5 mol % significantly decreased the catalyst performance. **Ir-3** was chosen as the precatalyst for investigating the scope of the transfer hydrogenation process over **Ir-4**, due to the significantly lower synthesis yield of the latter, although both complexes showed comparable catalytic activity (Table 3).

Subsequently, the scope and limitations of our protocol were evaluated by using a series of ketones and aldehydes with the above optimized reaction conditions. Aromatic ketones could be reduced in excellent yields. The catalyst showed a relatively low activity toward acetophenones with electron-donating substituents. The catalytic activity increased with increasing electron-withdrawing nature of the para substituent. Halogenated aromatic ketones with −F, −Br, and −CF₃ consistently afforded the corresponding alcohols in excellent yields. Sterically encumbered ketone also afforded the desired alcohol in good yields. Of interest was the effective transfer hydrogenation of heteroaromatic ketones such as furyl-based ketones, which present a greater challenge due to the potential coordination of heteroatoms to the metal center. In addition to the reduction of saturated aryl ketones, the transfer hydrogenation of α,β-unsaturated ketone and sterically hindered ketones demonstrated excellent functional group compatibility.

Complex **Ir-3** also shows high catalytic activity for the transfer hydrogenation of aldehydes. Normally, aldehydes tend to undergo the Cannizzaro reaction in the presence of many transfer hydrogenation catalysts, but no such products were detected in our case.

Bäckvall, Andersson, and co-workers have described both the monohydride and dihydride pathways in catalytic transfer hydrogenation reactions.[10] To distinguish between the monohydride and dihydride pathways, the transfer hydrogenation of acetophenone was carried out in the presence of

Table 3. Transfer Hydrogenation of Various Ketones and Aldehydes with Catalyst Ir-3[a]
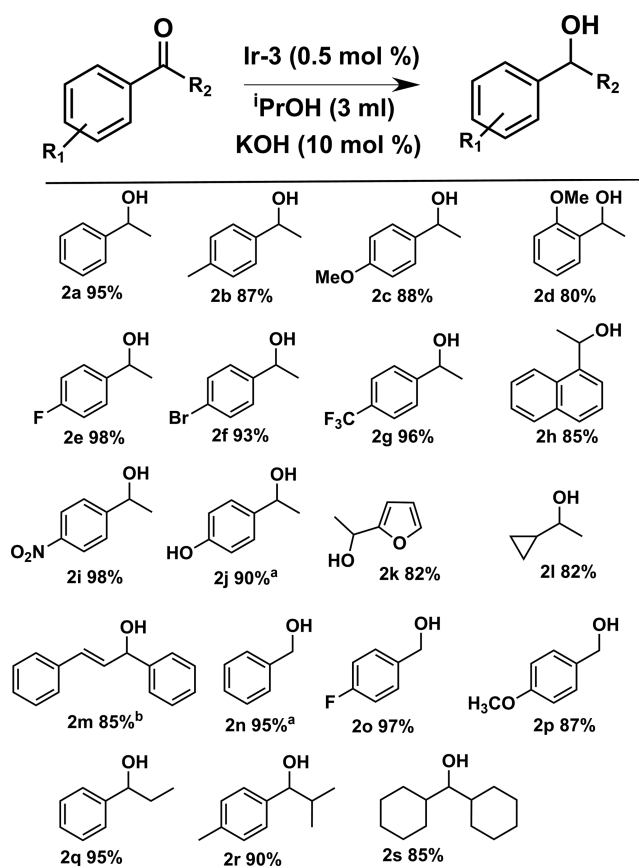
[a]Unless otherwise stated, yields refer to isolated products. Reaction conditions: substrate (0.25 mmol) in 3 mL of isopropanol at 100°C, catalyst precursor (0.5 mol %), base (10 mol %). Yield measured by ¹H NMR spectroscopy using hexamethylbenzene as an internal standard. [b]Using 1 mol % catalyst.

isopropanol-OD as the hydride source. For the dihydride pathway, one would expect the incorporation of deuterium in both C−H and O−H positions (Figure 5). However, no
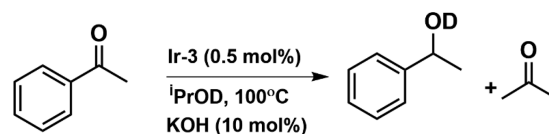
Figure 5. Deuterium-labeling experiment.

noticeable deuterium incorporation was observed in the benzylic C−H position (Figure S16), suggesting that transfer hydrogenation occurs via the monohydride pathway.[35]

The mechanism of transfer hydrogenation is thought to proceed through the formation of metal hydride species.[36] When a solution of precatalyst **Ir-3** in isopropanol was heated in the presence of KOH at 100 °C, a hydride resonance was detected at −13.7 ppm by NMR, demonstrating the formation of metal hydrides during the catalytic cycle (Figures S14 and S15). A plausible mechanism is suggested based on one proposed for Noyori type catalysts with N−H ligands (Scheme 3).[16] As suggested by Noyori and co-workers, treatment of precursor complex **Ir-3** with a base such as KOH first leads to the loss of the chloride ligand, resulting in the formation of

Scheme 3. Plausible Mechanism for the Transfer Hydrogenation of Ketones with N^N-Chelated Iridium Complex Ir-3
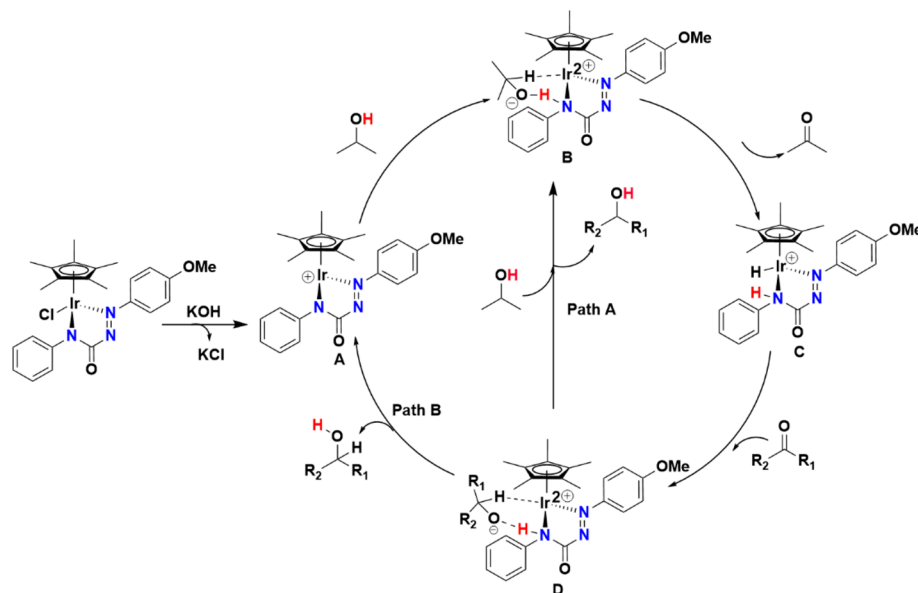
unsaturated complex **A** with 16 valence electrons. Intermediate **A** uptakes an OH proton from isopropanol resulting in the formation of intermediate **B** with a protonated azocarboxamide ligand. Further stepwise uptake of a hydride from isopropanol leads to the formation of 18-electron monohydride intermediate **C** along with the corresponding ketone. Intermediate **C** further transfers the hydride to the preorganized substrate through intermolecular H-bonding of the N−H moiety, leading to the formation of intermediate **D**. Hydride transfer to another ketone and proton transfer from the ligand results in the reformation of **A** and the corresponding alcohol. Although different mechanisms based on different transition states have been discussed, the involvement of **A** and **C** as the key catalytic intermediates is common to all these scenarios reported so far.[37,38]

Upon heating all iridium complexes in the presence of isopropanol and KOH, metal hydride resonances were detected by NMR in all cases (Figures S14 and S15). Therefore, the steps leading to the formation of iridium hydride from **Ir-3** (N^N-chelated iridium complex) would be similar to those for the other N^O- and N^C-chelated iridium complexes. The reactivity differences between N^N-, N^O-, and N^C-chelated iridium complexes could be due to the efficiency of hydride transfer leading to the facile formation of the hydrido complex in the presence of 2-propanol.[39]

3. CONCLUSION

In summary, we have demonstrated that an N^N- or N^O- or N^C-chelated half-sandwich iridium complex can be selectively synthesized from the reaction of an azocarboxamide ligand with [Cp*IrCl₂]₂ by simply changing the reaction conditions.

2-(4-Methoxyphenyl)-N-phenyldiazenecarboxamide ligand **L2** afforded both N^N-chelated mononuclear (**Ir-3**) and N^N- and N^C-chelated diiridium complexes (**Ir-4**) by reactions with [Cp*IrCl₂]₂ and base. However, the same ligand gave only the N^C-chelated mononuclear iridium complex (**Ir-5**) in the presence of NH₄PF₆. C−H activation was observed for both **Ir-4** and **Ir-5** complexes at the phenyl ring. While **Ir-5** exhibits only one N^C donor set, binuclear iridium complex **Ir-4** shows an unprecedented coordination

motif of the azocarboxamide with both N^N and N^C donor sets.

However, N,2-diphenyldiazenecarboxamide ligand **L1** afforded only the mononuclear N^N-chelated complex (**Ir-1**) upon reaction with [Cp*IrCl₂]₂ and base and mononuclear N^O-chelated iridium complex **Ir-2** in the presence of NH₄PF₆. No C−H activation was observed at the phenyl. All these complexes were investigated electrochemically and by spectroscopic methods.

All complexes under investigation were tested in transfer hydrogenation catalysis. When comparing their reactivity in transfer hydrogenation, a prominent effect of the variable mode of chelation on their reactivity was observed. While the N^N (amide) chelated iridium complexes showed the highest reactivity, the lowest activity was observed for the mononuclear N^C-chelated iridium complex, in which the amide group is not directly connected to the metal center. Therefore, the incorporation of the amide N−H group in close proximity to the metal center is highly recommended for the transfer hydrogenation catalyst. We have shown here how the introduction of a remote methoxy group on the ligand periphery can have a decisive effect on the C−H activation at the ligand, the formation of various coordination modes and mononuclear versus dinuclear complexes, as well as on the activity of the resulting complexes in catalytic transfer hydrogenation reactions. It is intriguing that such a small and synthetically simple modification of the ligand can have a dramatic effect on the coordination modes and catalytic properties of the resulting metal complexes. Future work will aim to exploit these small modifications to create metal complexes with tailored properties.

4. EXPERIMENTAL SECTION

4.1. General Procedures and Materials. Commercially available chemicals were used without further purification. All solvents were dried with appropriate drying agents, distilled, and degassed by standard techniques prior to use. Azocarboxamide ligands **L1** and **L2** were synthesized according to literature procedures.[3,40] ¹H NMR spectra were recorded with Bruker AV 250, Jeol ECS 400, and JEOL ECZ 400R spectrometers at 25 °C. Some ¹H and ¹³C spectra were recorded with a Bruker Avance III 500 MHz instrument at 23

°C. Chemical shifts are reported in ppm relative to tetramethylsilane or with reference to the residual solvent peaks. Mass spectrometry was performed on an Agilent 6210 ESI-TOF. Cyclic voltammograms were recorded with a PAR VersaStat 4 potentiostat (Ametek) by working in freshly distilled and degassed dichloromethane (DCM; anhydrous, VWR) and acetonitrile with 0.1 M NBu$_4$PF$_6$ (dried, >99.0%, electrochemical-grade, Fluka) as electrolyte. A three-electrode setup was used with glassy carbon as the working electrode, coiled platinum wire as the counter electrode, and coiled silver wire as the pseudoreference electrode. The ferrocene/ferrocenium couple was used as internal reference.

UV/vis−NIR spectra were recorded with an Avantes spectrometer consisting of a light source (AvaLightDH-S-Bal), a UV/vis detector (AvaSpec-ULS2048), and an NIR detector (AvaSpec-NIR256-TEC). Spectroelectrochemical measurements were performed in an optically transparent thin-layer electrochemical (OTTLE) cell[41] (CaF$_2$ windows) with a platinum mesh working electrode, a platinum mesh counter electrode, and a silver foil pseudoreference electrode. EPR spectra at X-band frequency (ca. 9.5 GHz) were obtained with a Magnettech MS-5000 benchtop EPR spectrometer equipped with a rectangular TE 102 cavity and TC HO4 temperature controller. The measurements were performed in synthetic quartz glass tubes. For EPR spectroelectrochemistry, a three-electrode setup was employed using two Teflon-coated platinum wires (0.005 in. bare, 0.008 in. coated) as the working and counter electrodes and a Teflon-coated silver wire (0.005 in. bare, 0.007 in. coated) as the pseudoreference electrode.

Single-crystal X-ray diffraction data were collected on a Bruker D8 Venture system at 100(2) K using graphite-monochromated Mo Kα radiation (λα = 0.710 73 Å). The strategy for the data collection was evaluated by using the APEX2 software. The data were collected by ω- and φ-scan techniques and scaled and reduced using the APEX2 and SADABS software. The structures were solved by intrinsic phasing or direct methods using SHELXT-2014/5 and refined using SHELXL-2014/7 by full-matrix least-squares, refining on F^2. Non-hydrogen atoms were refined anisotropically.[42]

4.2. Synthesis of Complex Ir-1. The Ir precursor [Cp*IrCl$_2$]$_2$ (79.7 mg, 0.1 mmol, 1 equiv) was dissolved in dichloromethane (10 mL), and then *N*,2-diphenyldiazenecarboxamide **L1** (45.1 mg, 0.2 mmol, 2 equiv) and triethylamine (0.2 mL, 1.4 mmol, 14 equiv) were added to the solution. The reaction mixture was stirred for 24 h at room temperature. The solvent was dried under high vacuum and then further purified over basic alumina (5 wt %) with a DCM/MeCN gradient (1:0−1:1). The green product was isolated as the third fraction (45 mg, 0.08 mmol, 38%). The single crystal was grown up from a mixture of dichloromethane and hexane.

^{1}H NMR (400 MHz, CDCl$_3$) δ 7.96−7.92 (m, 2H, H2/H6), 7.68−7.64 (m, 2H, H2′/H6′), 7.54−7.50 (m, 3H, H3/H4/H5), 7.34−7.29 (m, 2H; H3′/H5′), 7.16−7.11 (m, 1H, H4′), 1.21 (s, 15H, (CH$_3$)10′−50′) ppm. ^{13}C NMR (400 MHz, CDCl$_3$) δ 132.82 (C4), 128.76 (C3/C5), 128.57 (C3′/C5′), 125.90 (C2′/C6′), 125.18 (C4′), 124.16 (C2/C6), 8.28 (C10′−50′) ppm. HR-MS (ESI) Calcd C$_{23}$H$_{25}$ClIrN$_3$O ([M + H]$^+$) *m/z* 588.141. Found: 588.134. Anal. Calcd: C$_{23}$H$_{25}$ClIrN$_3$O: C, 47.05; H, 4.29; N, 7.16. Found: C, 47.12; H, 4.30; N, 7.14.

4.3. Synthesis of Complex Ir-2. The Ir precursor [Cp*IrCl$_2$]$_2$ (79.7 mg, 0.1 mmol, 1 equiv) was dissolved in acetonitrile (6 mL) and ammonium hexafluorophosphate (32.6 mg, 0.2 mmol, 2 equiv) added to it. The solution was stirred at room temperature for 1 h. Then the yellow solution was filtered and added into the solution of *N*,2-diphenyldiazenecarboxamide (45.1 mg, 0.2 mmol, 2 equiv) in acetonitrile (6 mL), and the mixture was refluxed for 24 h. The solvent was dried under high vacuum and then further purified over basic alumina (5 wt %) with a DCM/MeCN gradient (1:0−1:1). The green product isolated as the first fraction, **Ir-2** (56.5 mg, 0.08 mmol, 39%), was recrystallized from DCM/hexane (1:2) and stored in the refrigerator. The single crystal was obtained by slow evaporation from a mixture of dichloromethane and hexane.

^{1}H NMR (400 MHz, CDCl$_3$) δ 9.55 (s, 1H, NH), 8.42−8.38 (m, 1H, H2), 7.99−7.95 (m, 1H, H6), 7.69−7.64 (m, 2H, H2′/H6′),

7.44−7.37 (m, 2H, H3/H5), 7.31−7.22 (m, 3H, H3″/H4″H5′), 7.21−7.16 (m, 1H, H4), 1.74 (s, 15H, (CH$_3$)10′−50′) ppm. ^{13}C NMR (400 MHz, CDCl$_3$) δ 134.90 (C6), 134.46 (C3′/C5′), 132.38 (C2), 129.47 (C3/C5), 125.06 (C4), 124.14 (C4′), 119.38 (C2′/C6′), 9.24 (C10′−50′) ppm. HR-MS (ESI) Calcd C$_{23}$H$_{26}$ClIrN$_3$O: ([M]$^+$): *m/z* 588.1381. Found: 588.1392. Anal. Calcd: C$_{23}$H$_{26}$ClIrN$_3$OPF$_6$: C, 37.68; H, 3.57; N, 5.73. Found: C, 37.12; H, 3.30; N, 5.64.

4.4. Synthesis of Complex Ir-3. The Ir precursor [Cp*IrCl$_2$]$_2$ (79.7 mg, 0.1 mmol, 1 equiv) was dissolved in DCM (10 mL) and mixed with 2-(4-methoxyphenyl)-*N*-phenyldiazenecarboxamide (51.1 mg, 0.2 mmol, 2 equiv), and trimethylamine (0.2 mL, 1.4 mmol, 14 equiv) was added. The reaction mixture was left for 2 h at room temperature stirred and then the solvent removed under high vacuum. The solid was purified with a DCM/MeCN gradient (1:0−1:1) over basic aluminum oxide (5 wt %). The green product 6.1 (38 mg, 0.06 mmol, 30%) isolated as the third fraction was recrystallized from DCM/hexane (1:2) mixture and stored in the refrigerator.

^{1}H NMR (400 MHz, CDCl$_3$) δ 8.05−7.98 (m, 2H, H2/H6), 7.72−7.67 (m, 2H, H2′/H6′), 7.35−7.29 (m, 2H, H3′/H5′), 7.16−7.10 (m, 1H, H4′), 7.02−6.95 (m, 2H, H3/H5), 3.92 (s, 3H, OMe), 1.26 (s, 15H, (CH$_3$)10′−50′) ppm. ^{13}C NMR (400 MHz, CDCl$_3$) δ 128.44 (C3′/C5′), 126.57 (C2/C6), 125.90 (C2′/C6′), 124.91 (C4′), 113.62 (C3/C5), 55.84 (OMe), 8.26 (C10′−50′) ppm. HR-MS (ESI) Calcd C$_{24}$H$_{27}$ClIrN$_3$O$_2$ ([M]$^+$): *m/z* 618.1486. Found: 618.1493. Anal. Calcd: C$_{24}$H$_{27}$ClIrN$_3$O$_2$: C, 46.71; H, 4.41; N, 6.81. Found: C, 46.78; H, 4.44; N, 6.91.

4.5. Synthesis of Complex Ir-4. The Ir precursor [Cp*IrCl$_2$]$_2$ (33.1 mg, 0.05 mmol, 1 equiv) was dissolved in DCM (12 mL) and mixed with 2-(4-methoxyphenyl)-*N*-phenyldiazenecarboxamide (25.5 mg, 0.1 mmol, 2 equiv), and triethylamine (0.2 mL, 1.4 mmol, 14 equiv) was added. The reaction mixture was left for 24 h at room temperature stirred, and then the solvent was removed in a high vacuum. The solid was purified with a DCM/MeCN gradients (1:0−1:1) over basic aluminum oxide (5 wt %) by column chromatography. The red product 6.2 (7.5 mg, 0.05 mmol, 15%) was isolated as the first fraction.

^{1}H NMR (400 MHz, CDCl$_3$) δ 8.38 (d, *J* = 9.0 Hz, 1H, H6), 7.92−7.89 (m, 2H, H2′/H6′), 7.42 (d, *J* = 2.6 Hz, 1H, H3), 7.31−7.26 (m, 2H, H3′/H5′), 7.09−7.04 (m, 1H, H4′), 6.83 (dd, *J* = 9.1, 2.6 Hz, 1H, H5), 4.01 (s, 3H, OMe), 1.82 (s, 15H, (CH$_3$)10′−50′), 1.29 (s, 15H, (CH$_3$)10″−50″) ppm. ^{13}C NMR (400 MHz, CDCl$_3$) δ 132.85 (C6), 128.41 (C3′/C5′), 126.54 (C2′/C6′), 124.09 (C4′), 115.72 (C3), 112.95 (C5), 55.75 (OMe), 9.81 (C10′−50′), 8.10 (C10″−50″) ppm. HR-MS (ESI) Calcd C$_{34}$H$_{41}$Cl$_2$Ir$_2$N$_3$O$_2$ ([M − Cl]$^-$): *m/z* 944.215. Found: 944.214. Anal. Calcd: C$_{34}$H$_{41}$Cl$_2$Ir2N$_3$O$_2$: C, 41.71; H, 4.22; N, 4.29. Found: C, 41.37; H, 4.13; N, 4.59.

4.6. Synthesis of Complex Ir-5. The Ir precursor [Cp*IrCl$_2$]$_2$ (39.9 mg, 0.05 mmol, 1 equiv) was dissolved in acetonitrile (6 mL) and mixed with ammonium hexafluorophosphate (15.8 mg, 0.1 mmol, 2 equiv). The solution will last for an hour stirred at room temperature. The yellow solution was then filtered and transferred to a second solution from 2-(4-methoxyphenyl)-*N*-phenyldiazenecarboxamide (25.5 mg, 0.1 mmol, 2 equiv) in acetonitrile (6 mL). The reaction mixture was refluxed for 24 h. The solvent was removed under a high vacuum, and the red solid was purified by column chromatography over basic aluminum oxide (5 wt %) with a DCM/MeCN gradient (1:0−1:1). The first fraction was isolated as green product 6.3 (27.3 mg, 0.04 mmol, 36%), recrystallized in DCM/hexane (1:2), and stored in the refrigerator.

^{1}H NMR (400 MHz, CDCl$_3$) δ 9.56 (s, 1H, NH), 8.32 (d, *J* = 8.8 Hz, 1H, H6), 7.67 (dd, *J* = 8.6, 1.1 Hz, 2H, H2′/H6′), 7.46−7.37 (m, 3H, H3/H3′/H5′), 7.19−7.13 (m, 1H, H4′), 6.84 (dd, *J* = 8.8, 2.6 Hz, 1H, H5), 3.99 (s, 3H, OMe), 1.75 (s, 15H, (CH$_3$)10′−50′) ppm. ^{13}C NMR (400 MHz, CDCl$_3$) δ 134.73 (C6), 129.36 (C3′/C5′), 124.69 (C4′), 119.29 (C2′/C6′), 117.95 (C3), 112.18 (C5), 55.67 (OMe), 9.21 (C10′−50′) ppm. HR-MS (ESI) Calcd C$_{24}$H$_{27}$ClIrN$_3$O$_2$ ([M − Cl]$^-$): *m/z* 582.174. Found: 582.171. Anal. Calcd:

$C_{24}H_{27}ClIrN_3O_2$: C, 46.71; H, 4.41; N, 6.81. Found: C, 46.62; H, 4.40; N, 6.83.

4.7. General Procedure for Transfer Hydrogenation Catalysis. Benzophenone, the metal complex, and KOH were placed in a Schlenk flask. The flask was evacuated and flushed with nitrogen. Dry iPrOH was added, and the closed flask was heated to 100 °C. After the indicated reaction time the solvent was evaporated under reduced pressure. Hexamethylbenzene (0.1 equiv relative to the substrate) was added, and the yield was measured by ^1H NMR in $CDCl_3$. The amount of diphenylmethanol was calculated by the integration of the methine signal at 5.80 ppm (1H) and comparison to the standard signal at 2.24 ppm (18H). As a control the remaining amount of benzophenone was calculated by the integral of the benzophenone signal at 7.80 ppm (4H).

For the substrate scope, metal complex **Ir-3** (0.5 mol %), respective aldehydes or ketones (0.5 mmol), and KOH (10 mol %) were placed in a Schlenk flask. The flask was evacuated and flushed with nitrogen. iPrOH (3 mL) was added, and the closed flask was heated to 100 °C for 20 h. The solvent was evaporated under reduced pressure, and the crude product was purified by silica column chromatography.

4.8. Metal Hydride Formation. The respective metal complex (5 mg) was dissolved in dry, degassed iPrOH (5 mL) under an inert atmosphere of nitrogen. The resulting solution was heated to 100 °C in a closed flask. After 10 h, the solvent was evaporated under reduced pressure at ambient temperature. The resulting solid was dissolved in dry degassed CD_2Cl_2 (0.8 mL), and the ^1H NMR spectrum was recorded under a nitrogen atmosphere.

ASSOCIATED CONTENT

Ⓢ Supporting Information

The Supporting Information is available free of charge at https://pubs.acs.org/doi/10.1021/acs.organomet.1c00468.

> Crystallographic data for complexes **Ir-1−Ir-5**, spectroscopic data for complexes **Ir-1−Ir-5**, characterization data for the catalytic products (PDF)

Accession Codes

CCDC 2068800−2068802 contain the supplementary crystallographic data for this paper. These data can be obtained free of charge via www.ccdc.cam.ac.uk/data_request/cif, or by emailing data_request@ccdc.cam.ac.uk, or by contacting The Cambridge Crystallographic Data Centre, 12 Union Road, Cambridge CB2 1EZ, UK; fax: +44 1223 336033.

AUTHOR INFORMATION

Corresponding Authors

> **Janez Košmrlj** − *Faculty of Chemistry and Chemical Technology, University of Ljubljana, SI-1000 Ljubljana, Slovenia;* ⊙ orcid.org/0000-0002-3533-0419;
> Email: janez.kosmrlj@fkkt.uni-lj.si
>
> **Biprajit Sarkar** − *Lehrstuhl für Anorganische Koordinationschemie, Institut für Anorganische Chemie, Universität Stuttgart, D-70569 Stuttgart, Germany; Institut für Chemie und Biochemie, Freie Universität Berlin, D-14195 Berlin, Germany;* ⊙ orcid.org/0000-0003-4887-7277;
> Email: biprajit.sarkar@iac.uni-stuttgart.de

Authors

> **Shubhadeep Chandra** − *Lehrstuhl für Anorganische Koordinationschemie, Institut für Anorganische Chemie, Universität Stuttgart, D-70569 Stuttgart, Germany*
>
> **Ola Kelm** − *Institut für Chemie und Biochemie, Freie Universität Berlin, D-14195 Berlin, Germany*
>
> **Uta Albold** − *Institut für Chemie und Biochemie, Freie Universität Berlin, D-14195 Berlin, Germany*

> **Arijit Singha Hazari** − *Lehrstuhl für Anorganische Koordinationschemie, Institut für Anorganische Chemie, Universität Stuttgart, D-70569 Stuttgart, Germany*
>
> **Damijana Urankar** − *Faculty of Chemistry and Chemical Technology, University of Ljubljana, SI-1000 Ljubljana, Slovenia*

Complete contact information is available at:
https://pubs.acs.org/10.1021/acs.organomet.1c00468

Notes

The authors declare no competing financial interest.

REFERENCES

(1) Sommer, M. G.; Marinova, S.; Krafft, M. J.; Urankar, D.; Schweinfurth, D.; Bubrin, M.; Košmrlj, J.; Sarkar, B. Ruthenium Azocarboxamide Half-Sandwich Complexes: Influence of the Coordination Mode on the Electronic Structure and Activity in Base-Free Transfer Hydrogenation Catalysis. *Organometallics* **2016**, *35*, 2840−2849.

(2) Klein, J.; Beerhues, J.; Schweinfurth, D.; van der Meer, M.; Gazvoda, M.; Lahiri, G. K.; Košmrlj, J.; Sarkar, B. Versatile Coordination of Azocarboxamides: Redox-Triggered Change of the Chelating Binding Pocket in Ruthenium Complexes. *Chem. - Eur. J.* **2018**, *24*, 18020−18031.

(3) Sommer, M. G.; Kureljak, P.; Urankar, D.; Schweinfurth, D.; Stojanović, N.; Bubrin, M.; Gazvoda, M.; Osmak, M.; Sarkar, B.; Košmrlj, J. Combining arene-Ru with azocarboxamide to generate a complex with cytotoxic properties. *Chem. - Eur. J.* **2014**, *20*, 17296−17299.

(4) Kaim, W. Complexes with 2,2'-azobispyridine and related 'S-frame' bridging ligands containing the azo function. *Coord. Chem. Rev.* **2001**, *219−221*, 463−488.

(5) Samanta, S.; Ghosh, P.; Goswami, S. Recent advances on the chemistry of transition metal complexes of 2-(arylazo)pyridines and its arylamino derivatives. *Dalton Trans* **2012**, *41*, 2213−2226.

(6) Sarkar, B.; Hübner, R.; Pattacini, R.; Hartenbach, I. Combining two non-innocent ligands in isomeric complexes Pt(pap)(m)Q(n)(0) (pap = phenylazopyridine, Q = 3,5-di-tert-butyl-benzoquinone. *Dalton Trans* **2009**, 4653−4655.

(7) Shivakumar, M.; Pramanik, K.; Ghosh, P.; Chakravorty, A. Isolation and Structure of the First Azo Anion Radical Complexes of Ruthenium. *Inorg. Chem.* **1998**, *37*, 5968−5969.

(8) Doslik, N.; Sixt, T.; Kaim, W. The First Structural Characterization of an Azoaromatic Radical Anion Stabilized by Dicopper(I) Coordination. *Angew. Chem., Int. Ed.* **1998**, *37*, 2403−2404.

(9) Wang, D.; Astruc, D. The golden age of transfer hydrogenation. *Chem. Rev.* **2015**, *115*, 6621−6686.

(10) Samec, J. S. M.; Bäckvall, J.-E.; Andersson, P. G.; Brandt, P. Mechanistic aspects of transition metal-catalyzed hydrogen transfer reactions. *Chem. Soc. Rev.* **2006**, *35*, 237−248.

(11) Ghoochany, L. T.; Farsadpour, S.; Sun, Y.; Thiel, W. R. New N,N,N-Donors Resulting in Highly Active Ruthenium Catalysts for Transfer Hydrogenation at Room Temperature. *Eur. J. Inorg. Chem.* **2011**, *2011*, 3431−3437.

(12) Baratta, W.; Benedetti, F.; Del Zotto, A.; Fanfoni, L.; Felluga, F.; Magnolia, S.; Putignano, E.; Rigo, P. Chiral Pincer Ruthenium and Osmium Complexes for the Fast and Efficient Hydrogen Transfer Reduction of Ketones. *Organometallics* **2010**, *29*, 3563−3570.

(13) Zassinovich, G.; Mestroni, G.; Gladiali, S. Asymmetric hydrogen transfer reactions promoted by homogeneous transition metal catalysts. *Chem. Rev.* **1992**, *92*, 1051−1069.

(14) Peris, E.; Crabtree, R. H. Recent homogeneous catalytic applications of chelate and pincer N-heterocyclic carbenes. *Coord. Chem. Rev.* **2004**, *248*, 2239−2246.

(15) Gnanamgari, D.; Sauer, E. L. O.; Schley, N. D.; Butler, C.; Incarvito, C. D.; Crabtree, R. H. Iridium and Ruthenium Complexes with Chelating N-Heterocyclic Carbenes: Efficient Catalysts for Transfer Hydrogenation, *β*-Alkylation of Alcohols, and N-Alkylation of Amines. *Organometallics* **2009**, *28*, 321−325.

(16) Noyori, R. Asymmetric Catalysis: Science and Opportunities (Nobel Lecture) Copyright© The Nobel Foundation 2002. We thank the Nobel Foundation, Stockholm, for permission to print this lecture. *Angew. Chem., Int. Ed.* **2002**, *41*, 2008.

(17) Romain, C.; Gaillard, S.; Elmkaddem, M. K.; Toupet, L.; Fischmeister, C.; Thomas, C. M.; Renaud, J.-L. New Dipyridylamine Ruthenium Complexes for Transfer Hydrogenation of Aryl Ketones in Water. *Organometallics* **2010**, *29*, 1992−1995.

(18) Bolje, A.; Hohloch, S.; van der Meer, M.; Košmrlj, J.; Sarkar, B. Ru(II), Os(II), and Ir(III) complexes with chelating pyridyl-mesoionic carbene ligands: structural characterization and applications in transfer hydrogenation catalysis. *Chem. - Eur. J.* **2015**, *21*, 6756−6764.

(19) Maity, R.; Mekic, A.; van der Meer, M.; Verma, A.; Sarkar, B. Triply cyclometalated trinuclear iridium(III) and trinuclear palladium(II) complexes with a tri-mesoionic carbene ligand. *Chem. Commun.* **2015**, *51*, 15106−15109.

(20) Michon, C.; MacIntyre, K.; Corre, Y.; Agbossou-Niedercorn, F. Pentamethylcyclopentadienyl Iridium(III) Metallacycles Applied to Homogeneous Catalysis for Fine Chemical Synthesis. *ChemCatChem* **2016**, *8*, 1755−1762.

(21) Wang, C.; Xiao, J. Iridacycles for hydrogenation and dehydrogenation reactions. *Chem. Commun.* **2017**, *53*, 3399−3411.

(22) Royer, A. M.; Rauchfuss, T. B.; Wilson, S. R. Coordination chemistry of a model for the GP cofactor in the Hmd hydrogenase: hydrogen-bonding and hydrogen-transfer catalysis. *Inorg. Chem.* **2008**, *47*, 395−397.

(23) Mi, X.; Huang, M.; Zhang, J.; Wang, C.; Wu, Y. Regioselective palladium-catalyzed phosphonation of coumarins with dialkyl H-phosphonates via C-H functionalization. *Org. Lett.* **2013**, *15*, 6266−6269.

(24) Zhou, G.; Aboo, A. H.; Robertson, C. M.; Liu, R.; Li, Z.; Luzyanin, K.; Berry, N. G.; Chen, W.; Xiao, J. N,O- vs N,C-Chelation in Half-Sandwich Iridium Complexes: A Dramatic Effect on Enantioselectivity in Asymmetric Transfer Hydrogenation of Ketones. *ACS Catal.* **2018**, *8*, 8020−8026.

(25) Tajuddin, H.; Harrisson, P.; Bitterlich, B.; Collings, J. C.; Sim, N.; Batsanov, A. S.; Cheung, M. S.; Kawamorita, S.; Maxwell, A. C.; Shukla, L.; Morris, J.; Lin, Z.; Marder, T. B.; Steel, P. G. Iridium-catalyzed C−H borylation of quinolines and unsymmetrical 1,2-disubstituted benzenes: insights into steric and electronic effects on selectivity. *Chem. Sci.* **2012**, *3*, 3505.

(26) Semwal, S.; Ghorai, D.; Choudhury, J. Wingtip-Dictated Cyclometalation of N-Heterocyclic Carbene Ligand Framework and Its Implication toward Tunable Catalytic Activity. *Organometallics* **2014**, *33*, 7118−7124.

(27) Gorelsky, S. I.; Lapointe, D.; Fagnou, K. Analysis of the concerted metalation-deprotonation mechanism in palladium-catalyzed direct arylation across a broad range of aromatic substrates. *J. Am. Chem. Soc.* **2008**, *130*, 10848−10849.

(28) Davies, D. L.; Donald, S. M. A.; Al-Duaij, O.; Macgregor, S. A.; Pölleth, M. Electrophilic C-H activation at Cp*Ir: ancillary-ligand control of the mechanism of C-H activation. *J. Am. Chem. Soc.* **2006**, *128*, 4210−4211.

(29) Huang, S.; Hong, X.; Cui, H.-Z.; Zhan, B.; Li, Z.-M.; Hou, X.-F. Bimetallic Bis-NHC-Ir(III) Complex Bearing 2-Arylbenzo[d]-oxazolyl Ligand: Synthesis, Catalysis, and Bimetallic Effects. *Organometallics* **2020**, *39*, 3514−3523.

(30) Daw, P.; Ghatak, T.; Doucet, H.; Bera, J. K. Cyclometalations on the Imidazo[1,2-*a*][1,8]naphthyridine Framework. *Organometallics* **2013**, *32*, 4306−4313.

(31) Mazloomi, Z.; Pretorius, R.; Pàmies, O.; Albrecht, M.; Diéguez, M. Triazolylidene Iridium Complexes for Highly Efficient and Versatile Transfer Hydrogenation of C = O, C = N, and C = C Bonds and for Acceptorless Alcohol Oxidation. *Inorg. Chem.* **2017**, *56*, 11282−11298.

(32) Navarro, M.; Segarra, C.; Pfister, T.; Albrecht, M. Structural, Electronic, and Catalytic Modulation of Chelating Pyridylideneamide Ruthenium(II) Complexes. *Organometallics* **2020**, *39*, 2383−2391.

(33) Takehara, J.; Hashiguchi, S.; Fujii, A.; Inoue, S.; Ikariya, T.; Noyori, R. Amino alcohol effects on the ruthenium(II)-catalysed asymmetric transfer hydrogenation of ketones in propan-2-ol. *Chem. Commun.* **1996**, 233.

(34) Sato, Y.; Kayaki, Y.; Ikariya, T. Comparative Study of Bifunctional Mononuclear and Dinuclear Amidoiridium Complexes with Chiral C-N Chelating Ligands for the Asymmetric Transfer Hydrogenation of Ketones. *Chem. - Asian J.* **2016**, *11*, 2924−2931.

(35) Zhang, G.; Hanson, S. K. Cobalt-catalyzed transfer hydrogenation of C = O and C = N bonds. *Chem. Commun.* **2013**, *49*, 10151−10153.

(36) Hall, A. M. R.; Dong, P.; Codina, A.; Lowe, J. P.; Hintermair, U. Kinetics of Asymmetric Transfer Hydrogenation, Catalyst Deactivation, and Inhibition with Noyori Complexes As Revealed by Real-Time High-Resolution FlowNMR Spectroscopy. *ACS Catal.* **2019**, *9*, 2079−2090.

(37) Yamakawa, M.; Ito, H.; Noyori, R. The Metal−Ligand Bifunctional Catalysis: A Theoretical Study on the Ruthenium(II)-Catalyzed Hydrogen Transfer between Alcohols and Carbonyl Compounds. *J. Am. Chem. Soc.* **2000**, *122*, 1466−1478.

(38) Dub, P. A.; Ikariya, T. Quantum chemical calculations with the inclusion of nonspecific and specific solvation: asymmetric transfer hydrogenation with bifunctional ruthenium catalysts. *J. Am. Chem. Soc.* **2013**, *135*, 2604−2619.

(39) Ngo, A. H.; Ibañez, M.; Do, L. H. Catalytic Hydrogenation of Cytotoxic Aldehydes Using Nicotinamide Adenine Dinucleotide (NADH) in Cell Growth Media. *ACS Catal.* **2016**, *6*, 2637−2641.

(40) Cappoen, D.; Majce, V.; Uythethofken, C.; Urankar, D.; Mathys, V.; Kočevar, M.; Verschaeve, L.; Polanc, S.; Huygen, K.; Košmrlj, J. Biological evaluation of diazene derivatives as anti-tubercular compounds. *Eur. J. Med. Chem.* **2014**, *74*, 85−94.

(41) Heineman, W. R.; Burnett, J. N.; Murray, R. W. Optically transparent thin-layer electrodes: ninhydrin reduction in an infrared transparent cell. *Anal. Chem.* **1968**, *40*, 1974−1978.

(42) (a) *APEX2*; Bruker AXS Inc.: Madison, WI, 2012. (b) Sheldrick, G. M.. *SADABS, Program for Empirical Absorption Correction*, version 2008/1; University of Gottingen: Göttingen, Germany, 2008. (c) *SAINT+, Data Integration Engine*, version 8.27b; Bruker AXS Inc.: Madison, WI, 2012. (d) Sheldrick, G. M.. *SHELXL, Program for Crystal Structure Solution and Refinement*, version 2014/7; University of Göttingen: Göttingen, Germany, 2014. (e) Hübschle, C. B.; Sheldrick, G. M.; Dittrich, B. ShelXle: a Qt user interface for SHELXLirger. ShelXle: a Qt graphical user interface for SHELXL. *J. Appl. Crystallogr.* **2011**, *44*, 1281−1284. (f) Sheldrick, G. M. A short history of SHELX. *Acta Crystallogr., Sect. A: Found. Crystallogr.* **2008**, *A64*, 112−122. (g) Sheldrick, G. M. Crystal structure refinement with SHELXL. *Acta Crystallogr., Sect. C: Struct. Chem.* **2015**, *71*, 3−8.